

# PCCP

Accepted Manuscript



This is an *Accepted Manuscript*, which has been through the Royal Society of Chemistry peer review process and has been accepted for publication.

*Accepted Manuscripts* are published online shortly after acceptance, before technical editing, formatting and proof reading. Using this free service, authors can make their results available to the community, in citable form, before we publish the edited article. We will replace this *Accepted Manuscript* with the edited and formatted *Advance Article* as soon as it is available.

You can find more information about *Accepted Manuscripts* in the [Information for Authors](#).

Please note that technical editing may introduce minor changes to the text and/or graphics, which may alter content. The journal's standard [Terms & Conditions](#) and the [Ethical guidelines](#) still apply. In no event shall the Royal Society of Chemistry be held responsible for any errors or omissions in this *Accepted Manuscript* or any consequences arising from the use of any information it contains.

# Effects of Separation Distance on the Charge Transfer Interactions in Quantum Dot-Dopamine Assemblies

Xin Ji, Wentao Wang and Hedi Mattoussi

*Department of Chemistry and Biochemistry, 95 Chieftan Way, Florida State University,  
Tallahassee, Florida 32306, USA*

**KEYWORDS:** Quantum Dot, Dopamine, Flory Excluded Volume, Poly (ethylene glycol), Charge Transfer Interactions, Separation Distance

## ABSTRACT:

We explored the effects of changing the separation distance on the charge transfer interactions between luminescent QD and proximal dopamine (in QD-dopamine assemblies), and the ensuing photoluminescence quenching. The separation distance was controlled using a tunable size bridge between the QD and dopamine via a poly (ethylene glycol) (PEG) chain where the average number of monomers was discretely varied. Using steady-state and time-resolved fluorescence measurements, we found that the photoluminescence losses were substantially more pronounced for QD-dopamine complexes prepared with the shortest PEG bridge, but progressively decreased with increasing PEG size. We also found that the charge transfer interactions can be affected by the nature of capping ligand used. In particular, we found that interactions and PL quenching in these assemblies tracked the effects of separation distance, conjugate valence and the energy mismatch between the dopamine redox levels and QD energy levels, when a compact zwitterion was used to control the conjugate configuration. However, additional effects of shielding the access of reactive dopamine to amine groups on the QD surface, when a longer inert PEG ligand was used, were found to produce heterogeneous conjugates, alter the interactions and produce weaker PL quenching.

E-mail: mattoussi@chem.fsu.edu

**INTRODUCTION:**

Semiconductor quantum dots (QDs) possess several unique electronic and optical properties with size- and composition-tunable excitation and emission spectra.<sup>1-4</sup> Colloidal CdSe-ZnS core-shell QDs, for example, exhibit a remarkable resistance to photo- and chemical degradation, and they have large absorption cross-section combined with narrow emission profiles that span the visible spectrum.<sup>5-9</sup> These nanocrystals have large surface-to-volume ratio with a large fraction of their atoms arrayed at the surfaces. They are stabilized with capping molecules, which can be modified, allowing one to disperse them in various solution media. These capping molecules provide electronic passivation of the surface. The photoemission properties of these materials can be highly sensitive to the nature of the surface ligand and/or to interactions with proximal dyes, redox complexes and certain metal ions.<sup>10-15</sup> As a result, they offer excellent platforms for developing sensors based on energy transfer and/or charge transfer interactions.<sup>13-19</sup> Moreover, these systems offer great flexibility as control over the number of dyes and/or complexes brought in close proximity to the QD surface can be achieved. Combined with the ability to tune the particle size, separation distance and spectral overlap, QD-conjugated to fluorescent dyes (or proteins) and redox-active complexes provide a rich and challenging system to investigate and understand.

Over the past decade, several studies focusing on the fabrication of hybrid QD-assemblies where control over separation distance and conjugate architecture have been reported.<sup>18, 20-22</sup> In one example, David and co-workers probed the distance-dependent electron transfer between CdS QDs and TiO<sub>2</sub> nanoparticles coupled through the use of bifunctional mercaptoalkanoic acid bridges with varying alkyl chain lengths.<sup>21</sup> They attributed the measured changes in the QD spectroscopic properties to electron transfer from photoexcited CdS QDs to the linked TiO<sub>2</sub> nanoparticles.<sup>21</sup> They found that the electron transfer efficiency decreased dramatically with increasing alkyl chain length (due to increased interparticle separation). In another example, Zhao and co-workers explored the use of CdSe-ZnS QDs coupled to gold nanoparticles via a complementary oligonucleotide sequences to investigate the distance dependence of metal-enhanced QD fluorescence in QD-DNA-Au assemblies.<sup>23</sup> The assemblies were constructed by linking QDs to gold nanoparticles through complementary oligonucleotide sequences of varying size. They reported that ~2.5 enhancement in the QD emission for

separation distance of  $\sim 12$  nm.<sup>23</sup> In a third example, we have probed the PL quenching of CdSe-ZnS QDs conjugated to fluorescent gold nanoclusters in buffer media,<sup>22</sup> where we tested the effects of varying the spectral overlap and separation distance on the QD photoluminescence. In particular, we measured strong PL loss but no enhancement in the cluster emission.

Dopamine is a neurotransmitter that plays a significant role in the brain activity and behavior.<sup>24-26</sup> It transmits information from one neuron to the next through chemical signals, and is closely associated with reward-seeking behaviors (*e.g.*, addiction); drastic changes in dopamine levels are associated with dysfunctions of the nervous system (*e.g.*, low dopamine levels are measured for patient with Parkinson's disease).<sup>27-29</sup>

Interactions of dopamine and its derivatives with luminescent QDs have been explored by several groups, due to the complex redox interactions and potential relevance in biology.<sup>30-33</sup> QD-dopamine complexes also provide a great platform for investigating the charge transfer interactions where control over the energy mismatch between the QD conduction and valence bands and dopamine oxidation potentials, as well as the valence of the conjugate can be realized.<sup>32, 33</sup> For instance, we have previously explored the effects of tuning the redox coupling in hybrid assemblies by varying the pH of the buffer and QD size on the nature of the redox interactions and the ensuing changes in the QD optical and spectroscopic properties.<sup>32-34</sup>

In this report we investigate the effects of varying the separation distance on the efficiency of charge transfer (CT) interactions in QD-dopamine conjugates using steady-state and time-resolved fluorescence measurements. The separation distance is tuned via a polyethylene glycol (PEG) bridge with varying chain length, namely PEG<sub>200</sub>, PEG<sub>400</sub>, PEG<sub>600</sub> and PEG<sub>1000</sub>. The PEG bridge (part of the surface capping ligand) is sandwiched between a dihydrolipoic acid anchoring group and a terminal amine used for attaching the redox active dopamine (see Figure 1). The conjugate design is further combined with mixed ligand exchange to control the number of reactive groups per QD and the nature of the inert ligand used (a terminally-inert PEG<sub>750</sub> vs a compact zwitterion). We measured a PL quenching efficiency that closely tracked the conjugate valence, but more importantly strongly depended on the size of the PEG bridge used. Moreover, we found that the nature of the inert ligands used in the mixed surface cap affects the rate of charge transfer and the resulting PL quenching. For instance, we found that when the inert ligand was switched from a zwitterion-modified

dihydrolipoic acid (DHLA-ZW) to PEG<sub>750</sub>-OMe-appended dihydrolipoic acid (DHLA-PEG<sub>750</sub>-OMe) the larger PEG moieties shielded the access of dopamine to the amine groups on the QD surface, weakening the CT transfer interactions and producing lower PL quenching.

## RESULTS AND DISCUSSIONS

### Conjugate Design and Control of the QD-to-dopamine Separation Distance

Our conjugate design combines the use of mixed ligand exchange and lipoic acid appended with polyethyleneglycol moieties as means to control the separation distance between the QD and dopamine as well as the number of dopamines per conjugate. It also provides a symmetric conjugate made of several redox groups positioned at the same distance from the QD center. We carried out ligand exchange on the QDs using a mixture of 95% inert ligands and 5% DHLA-PEG-amine ligands having varying PEG bridges, PEG<sub>200</sub> (3 EG units), PEG<sub>400</sub> (8 EG units), PEG<sub>600</sub> (12 EG units), and PEG<sub>1000</sub> (20 EG units). We also used two sets of inert ligands: DHLA-ZW (molecular scale) and DHLA-PEG<sub>750</sub>-OMe (a short oligomer). The QDs capped with mixtures of 5% DHLA-PEG-NH<sub>2</sub> and 95% DHLA-PEG<sub>750</sub>-OCH<sub>3</sub> will be referred to as EG/amine-PEG-QDs, while those prepared using a mixture of 5% DHLA-PEG-NH<sub>2</sub> and 95% DHLA-ZW will be referred to as ZW/amine-PEG-QDs. QDs prepared with 100% DHLA-PEG<sub>750</sub>-OMe or 100% DHLA-ZW, referred to as neutral (i.e., non-reactive), were used for control experiments. Following phase transfer to water media, the nanocrystals were covalently coupled to dopamine-isothiocyanate (dopamine-ITC), via amine-to-ITC reaction, using molar excess of dopamine-ITC.<sup>33</sup> In addition, by varying the nature and size of the inert ligand (which represents 95% of the total surface cap) from DHLA-ZW to DHLA-PEG<sub>750</sub>-OMe we were able to investigate how the effects of shielding dopamine-ITC access to the amine groups on the QD surfaces can affect the PL quenching. Here, we anticipated that using DHLA-PEG<sub>750</sub>-OMe as the inert ligand would shield access of the dopamine-ITC to the amine groups on the QD surface, thus reducing the redox coupling efficiency and the ensuing changes in the QD PL. In contrast, the more compact DHLA-ZW ligand would permit easier access of dopamine-ITC to the QD surface, resulting in stronger interactions and higher quenching (see Figure 1). We should emphasize that coupling of the dopamine to the QDs is specifically driven by the reaction of ITC with the amine groups present

on the PEG coating.<sup>33</sup> Physisorption and/or non-specific stickiness on the nanocrystal surfaces are negligible, given the nature of the polyethylene glycol capping shell used, and as verified using control dispersions made of 100% methoxy-PEG-capped QDs.<sup>33, 34</sup>

## Steady-State and Time-resolved Fluorescence Measurements

### 1. QD-dopamine Conjugates Prepared with ZW/amine-PEG-QDs

Figure 2a-d shows representative PL spectra collected from several dispersions of red-emitting QD-dopamine conjugates prepared using various PEG bridges: ZW/amine-PEG<sub>1000</sub>-QDs (2a), ZW/amine-PEG<sub>600</sub>-QDs (2b), ZW/amine-PEG<sub>400</sub>-QDs (2c) and ZW/amine-PEG<sub>200</sub>-QDs (2d). The data show that a progressive PL loss is measured when the dopamine-ITC molar concentration is increased for all sets of QD-dopamine assemblies studied, an observation that is fully consistent with previous findings on QD-dye and QD-redox-complex assemblies.<sup>20, 30, 33, 35</sup> For the same set of QDs, the PL losses were largest for the shortest PEG bridge (PEG<sub>200</sub>) and decreased with increasing PEG size to reach their lowest values measured for the PEG<sub>1000</sub>. Furthermore, substantially larger PL losses were measured for the conjugates prepared using yellow-emitting QDs compared to their red-emitting counterparts (see Figure 2e-f). The PL quenching efficiency,  $E$ , data shown in Figure 2e-f were extracted from the steady-state fluorescence data, using the expression,  $E = 1 - F_{DA}/F_D$ , where  $F_{DA}$  and  $F_D$  designate the PL intensity measured for dispersions of QD-dopamine conjugates and QDs alone (control, without dopamine complexes), respectively. Images from selected dispersions of these conjugates under UV illumination, shown in Figure 2g-h, provide a visual confirmation of the effects of varying the separation distance (and valence) on the degree of PL losses. In particular, dispersions of yellow-emitting QDs prepared with PEG<sub>200</sub> bridge exhibits a near total quenching of the emission at all dopamine-to-QD ratios used.

The data on the quenching efficiency shown in Figure 2e and 2f indicate that the overall trend can be fit using an expression of the form:<sup>33</sup>

$$E = \frac{\alpha' C_{\text{dop}}}{\alpha' C_{\text{dop}} + K'} \quad (1)$$

where  $\alpha'$  and  $K'$  are parameters that depend on the relative alignment of the redox levels of the dopamine with respect to the energy levels of the QD and the separation distance, respectively. Such expression is consistent with a configuration where each conjugate is made of a central QD surrounded by several dopamines positioned at a fixed average separation distance,  $r$ , from the QD center (i.e., centro-symmetric conjugate, see Figure 1). The above behavior is consistent with the predicted expression for the dependence of  $E$  vs. valence,  $n$ , given by:<sup>13, 33</sup>

$$E = \frac{\alpha n}{\alpha n + K} \quad (2)$$

Here  $\alpha$ ,  $K$  are directly related (proportional) to  $\alpha'$  and  $K'$ , respectively.<sup>33</sup> The conversion from equation 1 (for  $E$  vs  $C_{\text{dop}}$ ) to equation 2 (for  $E$  vs  $n$ ) is permitted by the fact that the number of coupled dopamines per QD in the final assemblies is expected to be proportional to the concentration of dopamine-ITC used in the reaction; amine-to-ITC coupling obeys the first-order bimolecular reaction.<sup>36</sup> We should also note that heterogeneity in the conjugate valence is an intrinsic property of QD-conjugates, and ideally should be taken into account when analyzing the dependence of the quenching efficiency on the dopamine-to-QD ratio (valence,  $n$ ). In such case accounting for the heterogeneity is achieved using the Poisson statistics and fitting the quenching data using an equation of the form:<sup>37</sup>

$$E(N) = \sum_{n=1}^N p(N,n) E(n) \quad \text{with} \quad p(N,n) = N^n \frac{e^{-N}}{n!}, \quad (3)$$

where  $N$  is the average dopamine-to-QD ratio used and  $n$  is the exact number of dopamine groups attached to a single QD. The Poisson distribution function,  $p(N,n)$ , accounts for heterogeneity in the conjugate valence, and  $E(n)$  is given by equation 2 above.<sup>37</sup> We have found that fitting the quenching data using equation 3 (after converting the concentration dependence to valence dependence) provides minimal improvement in the data fit for the set of conjugates prepared using ZW/amine-PEG-QDs. Thus, fitting the data compiled in Figure 2e-f using equation 1 yields values for  $K'/\alpha'$  that depend on the bridge size and the QD size (band

gap), with  $K'/\alpha' = 69.4$  (PEG<sub>1000</sub>), 43.4 (PEG<sub>600</sub>), 32.3 (PEG<sub>400</sub>) and 9.7 (PEG<sub>200</sub>) for red-emitting ZW/amine-PEG-QD-dopamine conjugates; similarly we extracted values that are consistently smaller for the set of yellow-emitting ZW/amine-PEG-QD-conjugates:  $K'/\alpha' = 20.7$ , 10.8, 9.0 and 3.8, respectively. These findings clearly indicate that the quenching efficiencies are larger for smaller size QDs (those with wider band gap), due to a larger energy mismatch with the redox levels of dopamine.

The above steady-state data were further supported and complemented by time-resolved fluorescence measurements, where faster PL decays (indicative of a shortening in the QD PL lifetime) were observed for dispersions of QD-assemblies with increasing valences compared to the control sample ( $C_{\text{dop}} = 0$ ) (see Figures 3 and S3). Moreover, shorter lifetimes were measured for the smaller size QDs and shorter PEG bridges. The above time-resolved PL data can be used to extract estimates for the charge-transfer rate constant ( $k_{\text{CT}}$ ), defined as:<sup>18, 38,</sup>

39

$$k_{\text{CT}} = \frac{1}{\tau_{\text{DA}}} - \frac{1}{\tau_{\text{D}}} \quad (4)$$

Table 1 summarizes the experimental values for the yellow and red-emitting QD-dopamine conjugates prepared with various size PEG bridges and with a nominal dopamine-ITC:amine ratio of 7.5:1. There is a pronounced increase in  $k_{\text{CT}}$  from  $5.92 \times 10^7 \text{ s}^{-1}$  for PEG<sub>1000</sub> to  $5.43 \times 10^8 \text{ s}^{-1}$  for PEG<sub>200</sub> (i.e., nearly a 10-fold increase) measured for yellow-emitting QD-dopamine conjugates prepared using ZW/amine-PEG-QDs. In comparison, a less pronounced increase in the transfer rate constant was measured for conjugates prepared with the red-emitting QDs. This confirms that the charge transfer interactions are also strongly affected by the QD size, in addition to the separation distance. The yellow-emitting (smaller radius) QDs have a larger band gap and provide more favorable mismatch in the energy levels between nanocrystal and dopamines, promoting more efficient charge transfer interactions.

**Table 1.** Experimental values for the charge-transfer rate constant ( $k_{\text{CT}}$ ) for all four sets of yellow and red-emitting QD-dopamine conjugates prepared using ZW/amine-PEG-QDs extracted from the TR fluorescence data. The conjugates were prepared with a nominal dopamine-ITC:amine ratio of 7.5:1 in DI water.

	Yellow QDs; $\lambda_{\text{em}/\text{max}} = 573 \text{ nm}$			Red QDs; $\lambda_{\text{em}/\text{max}} = 610 \text{ nm}$		
Bridges	$\tau_D$ (ns)	$\tau_{\text{DA}}$ (ns)	$k_{\text{CT}}$ ( $\text{s}^{-1}$ )	$\tau_D$ (ns)	$\tau_{\text{DA}}$ (ns)	$k_{\text{CT}}$ ( $\text{s}^{-1}$ )
DHLA-PEG <sub>1000</sub> -NH <sub>2</sub>	20.01	9.16	$5.92 \times 10^7$	19.78	16.07	$1.17 \times 10^7$
DHLA-PEG <sub>600</sub> -NH <sub>2</sub>	20.20	4.81	$1.58 \times 10^8$	20.44	13.00	$2.80 \times 10^7$
DHLA-PEG <sub>400</sub> -NH <sub>2</sub>	21.00	3.46	$2.41 \times 10^8$	22.45	11.38	$4.33 \times 10^7$
DHLA-PEG <sub>200</sub> -NH <sub>2</sub>	20.38	1.69	$5.43 \times 10^8$	22.65	8.18	$7.81 \times 10^7$

## 2. QD-dopamine Conjugates Prepared with EG/amine-PEG-QDs

Figure 4a shows plots of the PL quenching efficiencies ( $E$  vs  $C_{\text{dop}}$ ) at the various PEG bridges for conjugates prepared using PEG<sub>750</sub>-methoxy as the inert ligand in the mixed surface design, together with fits using equation 1; yellow-emitting QD-conjugates are shown. The data show that there is a reasonable agreement between the PL quenching efficiencies measured for the present set and those shown in Figure 2f above for the larger size bridges (PEG<sub>1000</sub>, PEG<sub>600</sub> and PEG<sub>400</sub>), even though, the values measured for the EG/amine-PEG-QDs are consistently smaller than those measured for ZW/amine-PEG-QDs shown in Figure 2f. However, the data collected from dispersions of conjugates prepared with the shortest PEG bridge (PEG<sub>200</sub>) exhibit a rather unusual behavior with smaller measured quenching efficiencies that level off at higher  $C_{\text{dop}}$ . We also found that fitting the corresponding PL quenching data using equation 1 does not provide a good agreement with the data for PEG<sub>200</sub> (see dashed line in Figure 4a). We attribute this difference to the effects of shielding the dopamine-ITC access to the amine groups on QD surface when a full size PEG<sub>750</sub> is used as the inert ligands, which may produce smaller number of dopamine per conjugate and more heterogeneous valence. Such screening affects all sets of the QD-dopamine conjugates regardless of the bridge size. However, they would be more pronounced for the smaller PEG bridges, in particular for PEG<sub>200</sub>. We take into account the effects of heterogeneity in the conjugate valence for EG/amine-PEG<sub>200</sub>-QDs conjugates using Poisson correction (equation 3). Clearly, such correction provides a better fit for the quenching efficiency data as shown in Figure 4b (solid red line). No sensible improvement could be measured when fitting the other data shown in Figure 4b. Additional data on the steady-state and time-resolved fluorescence spectra of EG/amine-PEG-QD-conjugates dispersions are provided in the Supporting Information (Figures S4 and S5).

## Discussion and Mechanism for the QD Emission Quenching

There are three major findings that can be highlighted from our measurements: 1) The PL quenching efficiency strongly depends on the PEG bridge size (i.e., separation distance) between QDs and proximal dopamine, with higher efficiencies measured for QD-dopamine conjugates assembled with a shorter PEG moiety, and vice versa. In addition, for a given PEG size the efficiency tracks the conjugate valence. 2) We measured larger quenching efficiencies for the yellow-emitting QDs (smaller size) compared with their red-emitting (larger size) counterparts when the same size bridge was used. 3) The QD PL losses also depend on the type of mixed ligands used. By changing the size and the nature of the inert ligand, we were able to explore the effects of ligands shielding on the dopamine-ITC-to-amine coupling reaction and measured quenching efficiency. For instance, using mixed surface QDs prepared with 95% zwitterion promoted better access of the dopamine-ITC to the amine groups compared to the case where larger PEG<sub>750</sub>-methoxy were used.

We now discuss the above findings within the framework of charge transfer interactions between dopamine and photoexcited QDs. We have previously shown that in these assemblies a photoexcited QD interacts with two distinct species (the reduced catechol and the oxidized quinone) that coexist within the same conjugate, with: 1) electron transfer from the catechol to the valence band of the QD; and 2) electron transfer from conduction band of the QD to the oxidized quinone. These CT pathways are strongly affected by the medium pH, and combined they alter the electron-hole recombination, resulting in PL quenching of the QD.<sup>33, 34</sup> Here, we analyze the effects of varying the separation distance on the charge transfer interaction, by maintaining a fixed pH (at ~ pH 6.5) and valence. At this pH we estimate, based on the Henderson-Hasselbalch relation ( $\text{pH} = \text{pK}_a - \log_{10} [\text{catechol}/\text{quinone}]$ ) that the catechol-to-quinone molar ratio in the dispersion is ~1000-to-1; we used  $\text{pK}_a = 9.3$  for this estimate.<sup>40</sup> This implies that within the present conditions, pathway 1 plays a dominant role in the charge transfer interactions in QD-dopamine conjugates. We thus limit our analysis to interactions involving electron transfer (ET) from the catechol groups to the valence band of a photoexcited QD (i.e.,  $k_{\text{CT}} \equiv k_{\text{ET}}$ , see Figure 5a). We would like to stress that potential contribution of defects in the ZnS shell to the CT interactions between the dopamine and QDs are not at the origin of

the differences in PL changes measured for the two sets of QDs. The overall thickness of the ZnS shell is similar for both sets and the separation distances used account for all relevant contributions (core-shell radius and ligand structure, see below). The measured differences are mainly due changes in the energy mismatch between the QDs and proximal redox complex as discussed in our recent report.<sup>34</sup>

To exploit the data on the quenching efficiency and extract a correlation between ET interactions and the separation distance, we first develop an estimate for the PEG size using the concept of excluded volume interactions developed by Flory for flexible polymers in good solvent conditions.<sup>41</sup> Indeed, polyethylene glycol is a flexible polymer highly compatible with water. In good solvent conditions, a polymer chain exhibit a coil like conformation, due to a balance between the excluded-volume interactions, which tend to expand its random configuration, and elastic restoring forces, which reduce its 3-dimensional expansion (swelling). The resulting end-to-end distance,  $R_f$ , for the PEG chain can be given by:<sup>42-44</sup>

$$R_f = a(M)^{\frac{1}{5}} \quad (5)$$

Here,  $a$  and  $M$  respectively designate the monomer size (3.5 Å for an ethylene glycol), and the number of repeat units per chain. The corresponding size for the various PEG bridges used, along with corresponding center-to-center separation distance,  $r$ , anticipated for the yellow and red-emitting QD-dopamine conjugates are compiled in Table 2.

**Table 2.** Size for PEG bridges along with center-to-center separation distance extracted from conformation consideration detailed in the text.

	Ligands	Repeat Unit	$R_f$ (Å)	Center-to-center Distance*, $r$ (Å)	
				Yellow-emitting QDs	Red-emitting QDs
Reactive Ligands	DHLA-PEG <sub>200</sub> -NH <sub>2</sub>	3	6.8	47.8	53.8
	DHLA-PEG <sub>400</sub> -NH <sub>2</sub>	8	12.2	53.2	59.2
	DHLA-PEG <sub>600</sub> -NH <sub>2</sub>	12	15.5	56.5	62.5
	DHLA-PEG <sub>1000</sub> -NH <sub>2</sub>	20	21.1	62.1	68.1
Non-reactive Ligand	DHLA-PEG <sub>750</sub> -OME	15	17.8	55.8	61.8

\*The center-to-center separation distance ( $r$ ) was estimated by combining the QD radius, the PEG size based on the Flory excluded volume calculation and the size of the DHLA group and the ITC linker.

We now correlate the experimental charge transfer rates extracted from the fluorescence data shown in Table 1 to the theoretical model of electron-transfer between two states developed by Marcus in 1956.<sup>45</sup> This theory has been successfully used to describe photoinduced electron transfer processes for an array of systems, and more recently to describe the electron transfer interactions between semiconductor QDs (as donor) and metal oxide nanoparticles and/or redox molecules (as acceptors) by Kamat and co-workers and Lian and co-workers.<sup>46-48</sup>

Within this description, the electron transfer rate from a single donor state (here a catechol) to a continuum of acceptor states (such as the valence band of the QD) can be expressed as:<sup>47</sup>

$$k_{ET} = \frac{2\pi}{h} \frac{H^2}{\sqrt{4\pi\lambda k_B T}} e^{\left\{ \frac{-(\Delta G + \lambda^2)}{4\lambda k_B T} \right\}} \quad (6)$$

where  $k_B$  is Boltzmann constant,  $h$  is Planck's constant, and  $e$  is the elementary charge.  $\Delta G$  is the change in the free energy of the system (associated with energy level mismatch between the donor and acceptor and is independent of the bridge size),  $\lambda$  is the system reorganization energy and  $H$  is the electronic coupling strength between donor and acceptor states. This parameter  $H$  accounts for the dependence of  $k_{ET}$  on the separation distance. Thus, the only variable parameter in the across the bridge charge transfer interactions between the catechols and the valence band for a given size QDs is the electronic coupling strength ( $H$ );  $H$  is predicted to exponentially vary with the separation distance (see Figure 5b).<sup>49-52</sup>

$$H^2 = H^0 e^{-\beta r} \quad (7)$$

Here  $H^0$  is an electronic factor,  $r$  is the center-to-center distance, and  $\beta$  is a constant that primarily depends on the nature of the bridge molecule. Examples of  $\beta$  values reported in the literature include  $\beta = 1.0-1.4 \text{ \AA}^{-1}$  for  $ET$  in proteins,  $\beta = 0.8-1.0 \text{ \AA}^{-1}$  for  $ET$  in saturated hydrocarbon bridges and  $\beta = 0.7-1.3 \text{ \AA}^{-1}$  for  $ET$  in polyproline.<sup>50, 52</sup> The expression for  $k_{ET}$  can be

further simplified for a given set of QD-dopamine assemblies where all the parameters are fixed except the electronic coupling  $H^2$  to yield:

$$\ln(k_{ET}) = -\beta r + k_0 \quad (8)$$

where  $k_0$  is a prefactor that depends on the relative alignment of redox levels of the dopamine with respect to the energy levels of the QD ( $\Delta G$ ). Figure 5c shows a plot of  $\ln(k_{ET})$  vs  $r$ , using the data shown in Table 1 and 2 for the conjugates prepared with the yellow- and red-emitting QDs. A linear dependency is observed in both cases, in agreement with the predicted behavior from equation 8, confirming that the Marcus model for the ET process in these assemblies is valid. We further extracted values for  $\beta \cong 0.15$  and  $0.13 \text{ \AA}^{-1}$  for the yellow- and red-emitting ZW/amine-PEG-QD-conjugates, respectively. Conversely, larger  $k_0$  value is extracted for the yellow QD-conjugates ( $k_0 \cong 27.5$ ) than for red QD-conjugates ( $k_0 \cong 25.3$ ). The two main features that emerge from the above analysis are: (1) The values for  $\beta$  are comparable for both sets of QDs, which is anticipated for these assemblies, since the same PEG moieties were used as the bridge molecule. (2) The higher intercept for the yellow-emitting QD-conjugates results from the larger energy mismatch (essentially larger  $\Delta G$  between the oxidation potential of the catechol and valence band of the QDs).

## Conclusion

We have investigated the distance-dependence charge transfer interactions that take place in assemblies of QD-dopamine conjugates coupled via a poly (ethylene glycol) (PEG) chain with varying size. The QD PL quenching efficiency as verified by steady-state and time-resolved fluorescence measurements is found to strongly depend on the PEG bridges used, with substantially more pronounced PL losses measured for shorter separation distance and vice versa. We were able to successfully correlate the electron transfer rates,  $k_{ET}$ , extracted from the fluorescence data, to the Marcus electron transfer model. A clearly-defined exponential dependence of the charge transfer rate on the separation distance is measured for the two sets

of QDs. In addition to the effects of separation distance, we found that changing the QD size also affects the measured PL quenching.

We further explored the effects of shielding on the conjugate formation and the ensuing PL losses by comparing data collected using QDs prepared with a compact zwitterion ligands (as the majority inert cap) to those collected from assemblies prepared with a longer inert PEG. We found that PEG coating (larger) shields dopamine access to the reactive amine, resulting in more heterogeneous conjugates and weaker PL quenching. QD-dopamine conjugates prepared with tunable PEG bridges provide promising platforms for constructing biosensors that exploit the unique redox characteristics of dopamine, the size-tunable spectroscopic properties of the QDs and the flexibility afforded by a varying size inert PEG bridge. Such QD-dopamine conjugates assembled via a tunable size PEG bridge, a controllable valence, while using a zwitterion-capped QDs are also greatly promising for use in intracellular sensing and imaging. One promising idea worth pursuing is to use the recognition specificity of dopamine to certain metals ions and the cysteine amino acid to assemble specific biological sensors for in vitro and/or in vivo studies.<sup>53-55</sup>

**Acknowledgments.** The authors thank FSU, the National Science Foundation (Grant No. 1058957) and Pfizer for financial support.

**Supporting Information Available.** Additional experimental details on the experimental set up, data analysis, QD growth, ligand synthesis, ligand exchange, and coupling reaction and conjugate purification are provided. Information is available free of charge via the Internet at <http://pubs.acs.org>.

## References

1. Wang, C. J.; Shim, M.; Guyot-Sionnest, P., Electrochromic nanocrystal quantum dots. *Science* **2001**, *291*, 2390-2392.
2. Talapin, D. V.; Lee, J. S.; Kovalenko, M. V.; Shevchenko, E. V., Prospects of Colloidal Nanocrystals for Electronic and Optoelectronic Applications. *Chem. Rev.* **2010**, *110*, 389-458.
3. Smith, A. M.; Nie, S. M., Semiconductor Nanocrystals: Structure, Properties, and Band Gap Engineering. *Acc. chem. res.* **2010**, *43*, 190-200.
4. Klimov, V. I., *Nanocrystal quantum dots*. 2nd ed.; CRC Press: Boca Raton, 2010; p xv, 469 p.
5. Alivisatos, A. P., Semiconductor clusters, nanocrystals, and quantum dots. *Science* **1996**, *271*, 933-937.
6. Murray, C. B.; Kagan, C. R.; Bawendi, M. G., Synthesis and characterization of monodisperse nanocrystals and close-packed nanocrystal assemblies. *Ann. Rev. of Mater. Science* **2000**, *30*, 545-610.
7. Peng, X. G.; Manna, L.; Yang, W. D.; Wickham, J.; Scher, E.; Kadavanich, A.; Alivisatos, A. P., Shape control of CdSe nanocrystals. *Nature* **2000**, *404*, 59-61.
8. Yildiz, I.; Deniz, E.; Raymo, F. M., Fluorescence modulation with photochromic switches in nanostructured constructs. *Chem. Soc. Rev.* **2009**, *38*, 1859-1867.
9. Amelia, M.; Impellizzeri, S.; Monaco, S.; Yildiz, I.; Silvi, S.; Raymo, F. M.; Credi, A., Structural and size effects on the spectroscopic and redox properties of CdSe nanocrystals in solution: the role of defect states. *Chemphyschem* **2011**, *12*, 2280-8.
10. Medintz, I. L.; Clapp, A. R.; Mattoussi, H.; Goldman, E. R.; Fisher, B.; Mauro, J. M., Self-assembled nanoscale biosensors based on quantum dot FRET donors. *Nat. Mater.* **2003**, *2*, 630-638.
11. Sykora, M.; Petruska, M. A.; Alstrum-Acevedo, J.; Bezel, I.; Meyer, T. J.; Klimov, V. I., Photoinduced charge transfer between CdSe nanocrystal quantum dots and Ru-polypyridine complexes. *J. Am. Chem. Soc.* **2006**, *128*, 9984-9985.
12. Pons, T.; Medintz, I. L.; Sapsford, K. E.; Higashiya, S.; Grimes, A. F.; English, D. S.; Mattoussi, H., On the quenching of semiconductor quantum dot photoluminescence by proximal gold nanoparticles. *Nano Lett.* **2007**, *7*, 3157-3164.
13. Medintz, I. L.; Pons, T.; Trammell, S. A.; Grimes, A. F.; English, D. S.; Blanco-Canosa, J. B.; Dawson, P. E.; Mattoussi, H., Interactions between Redox Complexes and Semiconductor Quantum Dots Coupled via a Peptide Bridge. *J. Am. Chem. Soc.* **2008**, *130*, 16745-16756.
14. Mattoussi, H.; Palui, G.; Na, H. B., Luminescent quantum dots as platforms for probing in vitro and in vivo biological processes. *Adv. Drug. Deliver. Rev.* **2012**, *64*, 138-166.
15. Stewart, M. H.; Huston, A. L.; Scott, A. M.; Efros, A. L.; Melinger, J. S.; Gemmill, K. B.; Trammell, S. A.; Blanco-Canosa, J. B.; Dawson, P. E.; Medintz, I. L., Complex Forster Energy Transfer Interactions between Semiconductor Quantum Dots and a Redox-Active Osmium Assembly. *ACS Nano* **2012**, *6*, 5330-5347.
16. Snee, P. T.; Somers, R. C.; Nair, G.; Zimmer, J. P.; Bawendi, M. G.; Nocera, D. G., A ratiometric CdSe/ZnS nanocrystal pH sensor. *J. Am. Chem. Soc.* **2006**, *128*, 13320-13321.
17. Chen, Y.; Thakar, R.; Snee, P. T., Imparting nanoparticle function with size-controlled amphiphilic polymers. *J. Am. Chem. Soc.* **2008**, *130*, 3744-3745.

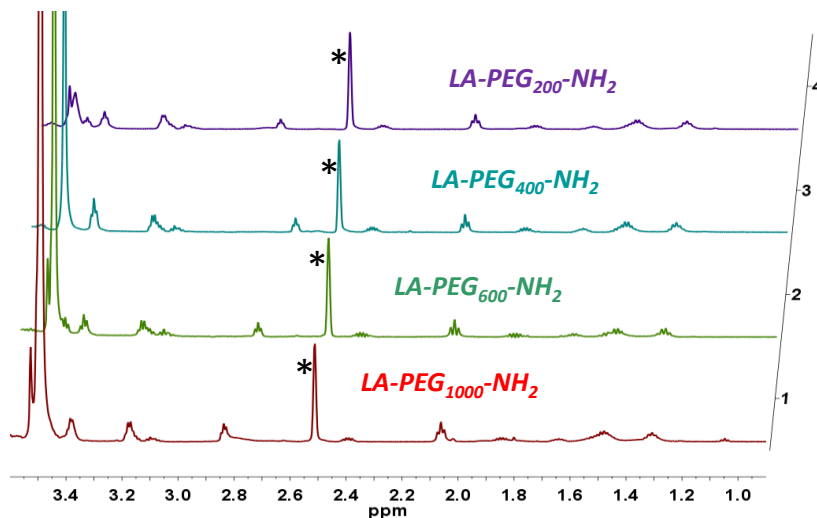
18. Robel, I.; Kuno, M.; Kamat, P. V., Size-dependent electron injection from excited CdSe quantum dots into TiO<sub>2</sub> nanoparticles. *J. Am. Chem. Soc.* **2007**, *129*, 4136-4137.
19. Freeman, R.; Finder, T.; Bahshi, L.; Gill, R.; Willner, I., Functionalized CdSe/ZnS QDs for the Detection of Nitroaromatic or RDX Explosives. *Adv. Mater.* **2012**, *24*, 6416-6421.
20. Clapp, A. R.; Medintz, I. L.; Mauro, J. M.; Fisher, B. R.; Bawendi, M. G.; Mattoussi, H., Fluorescence resonance energy transfer between quantum dot donors and dye-labeled protein acceptors. *J. Am. Chem. Soc.* **2004**, *126*, 301-310.
21. Dibbell, R. S.; Watson, D. F., Distance-Dependent Electron Transfer in Tethered Assemblies of CdS Quantum Dots and TiO<sub>2</sub> Nanoparticles. *J. Phys. Chem. C* **2009**, *113*, 3139-3149.
22. Aldeek, F.; Ji, X.; Mattoussi, H., Quenching of Quantum Dot Emission by Fluorescent Gold Clusters: What It Does and Does Not Share with the Forster Formalism. *J Phys Chem C* **2013**, *117*, 15429-15437.
23. Li, Y. Q.; Guan, L. Y.; Zhang, H. L.; Chen, J.; Lin, S.; Ma, Z. Y.; Zhao, Y. D., Distance-dependent metal-enhanced quantum dots fluorescence analysis in solution by capillary electrophoresis and its application to DNA detection. *Anal. Chem.* **2011**, *83*, 4103-9.
24. Gill, R.; Freeman, R.; Xu, J. P.; Willner, I.; Winograd, S.; Shweky, I.; Banin, U., Probing biocatalytic transformations with CdSe-ZnS QDs. *J. Am. Chem. Soc.* **2006**, *128*, 15376-15377.
25. Kovtun, O.; Tomlinson, I. D.; Sakrikar, D. S.; Chang, J. C.; Blakely, R. D.; Rosenthal, S. J., Visualization of the Cocaine-Sensitive Dopamine Transporter with Ligand-Conjugated Quantum Dots. *ACS Chem. Neurosci.* **2011**, *2*, 370-378.
26. Sedo, J.; Saiz-Poseu, J.; Busque, F.; Ruiz-Molina, D., Catechol-Based Biomimetic Functional Materials. *Adv. Mater.* **2013**, *25*, 653-701.
27. Vickrey, T. L.; Xiao, N.; Venton, B. J., Kinetics of the dopamine transporter in *Drosophila* larva. *ACS Chem Neurosci* **2013**, *4* (5), 832-7.
28. McFarland, K.; Spalding, T. A.; Hubbard, D.; Ma, J. N.; Olsson, R.; Burstein, E. S., Low dose bexarotene treatment rescues dopamine neurons and restores behavioral function in models of Parkinson's disease. *ACS Chem. Neurosci.* **2013**, *4*, 1430-8.
29. Li, Y.; Zhou, Y.; Qi, B.; Gong, T.; Sun, X.; Fu, Y.; Zhang, Z., Brain-Specific Delivery of Dopamine Mediated by N,N-Dimethyl Amino Group for the Treatment of Parkinson's Disease. *Molecular Pharmaceutics* **2014**, *11* (9), 3174-3185.
30. Clarke, S. J.; Hollmann, C. A.; Zhang, Z. J.; Suffern, D.; Bradforth, S. E.; Dimitrijevic, N. M.; Minarik, W. G.; Nadeau, J. L., Photophysics of dopamine-modified quantumdots and effects on biological systems. *Nat. Mater.* **2006**, *5*, 409-417.
31. Cooper, D. R.; Suffern, D.; Carlini, L.; Clarke, S. J.; Parbhoo, R.; Bradforth, S. E.; Nadeau, J. L., Photoenhancement of lifetimes in CdSe/ZnS and CdTe quantum dot-dopamine conjugates. *Phys. Chem. Chem. Phys.* **2009**, *11*, 4298-310.
32. Medintz, I. L.; Stewart, M. H.; Trammell, S. A.; Susumu, K.; Delehanty, J. B.; Mei, B. C.; Melinger, J. S.; Blanco-Canosa, J. B.; Dawson, P. E.; Mattoussi, H., Quantum-dot/dopamine bioconjugates function as redox coupled assemblies for in vitro and intracellular pH sensing. *Nat. Mater.* **2010**, *9*, 676-684.
33. Ji, X.; Palui, G.; Avellini, T.; Na, H. B.; Yi, C.; Knappenberger, K. L.; Mattoussi, H., On the pH-Dependent Quenching of Quantum Dot Photoluminescence by Redox Active Dopamine. Ruiz-Molina **2012**, *134*, 6006-6017.

34. Ji, X.; Makarov, N. S.; Wang, W.; Palui, G.; Robel, I.; Mattoussi, H., Tuning the Redox Coupling between Quantum Dots and Dopamine in Hybrid Nanoscale Assemblies. *J. Phys. Chem. C* **2015**, *119*, 3388-3399.
35. Dennis, A. M.; Bao, G., Quantum Dot-Fluorescent Protein Pairs as Novel Fluorescence Resonance Energy Transfer Probes. *Nano Lett.* **2008**, *8*, 1439-1445.
36. Sapsford, K. E. e. a., Kinetics of metal-affinity driven self-assembly between proteins or peptides and CdSe-ZnS quantum dots. *J. Phys. Chem. C* **2007**, *111*, 11528-11538.
37. Pons, T.; Medintz, I. L.; Wang, X.; English, D. S.; Mattoussi, H., Solution-phase single quantum dot fluorescence resonance energy transfer. *J. Am. Chem. Soc.* **2006**, *128*, 15324-15331.
38. Tvrdy, K.; Frantsuzov, P. A.; Kamat, P. V., Photoinduced electron transfer from semiconductor quantum dots to metal oxide nanoparticles. *P Natl Acad Sci USA* **2011**, *108*, 29-34.
39. Zhu, H.; Song, N.; Lian, T., Charging of quantum dots by sulfide redox electrolytes reduces electron injection efficiency in quantum dot sensitized solar cells. Ruiz-Molina **2013**, *135*, 11461-4.
40. Laviron, E., Electrochemical Reactions with Protonations at Equilibrium .10. The Kinetics of the Para-Benzoquinone Hydroquinone Couple on a Platinum-Electrode. *J Electroanal. Chem.* **1984**, *164*, 213-227.
41. Flory, P. J., *Principles of polymer chemistry*. Cornell University Press: Ithaca, 1953; p 672 p.
42. Degennes, P. G., Conformations of Polymers Attached to an Interface. *Macromolecules* **1980**, *13*, 1069-1075.
43. Degennes, P. G., Polymers at an Interface - a Simplified View. *Adv. Colloid. Interfac.* **1987**, *27*, 189-209.
44. Jokerst, J. V.; Lobovkina, T.; Zare, R. N.; Gambhir, S. S., Nanoparticle PEGylation for imaging and therapy. *Nanomedicine (Lond)* **2011**, *6*, 715-28.
45. Marcus, R. A., On the Theory of Oxidation-Reduction Reactions Involving Electron Transfer .1. *J. Chem. Phys.* **1956**, *24*, 966-978.
46. Sakata, T.; Hashimoto, K.; Hiramoto, M., New aspects of electron transfer on semiconductor surface: dye-sensitization system. *J. of Phys. Chem.* **1990**, *94*, 3040-3045.
47. Huang, J.; Stockwell, D.; Huang, Z. Q.; Mohler, D. L.; Lian, T. Q., Photoinduced ultrafast electron transfer from CdSe quantum dots to re-bipyridyl complexes. Ruiz-Molina **2008**, *130*, 5632-5633.
48. Tvrdy, K.; Frantsuzov, P. A.; Kamat, P. V., Photoinduced electron transfer from semiconductor quantum dots to metal oxide nanoparticles. *Proc Natl Acad Sci U S A* **2011**, *108*, 29-34.
49. Lewis, F. D.; Wu, T.; Zhang, Y.; Letsinger, R. L.; Greenfield, S. R.; Wasielewski, M. R., Distance-dependent electron transfer in DNA hairpins. *Science* **1997**, *277*, 673-6.
50. Davis, W. B.; Svec, W. A.; Ratner, M. A.; Wasielewski, M. R., Molecular-wire behaviour in p-phenylenevinylene oligomers. *Nature* **1998**, *396*, 60-63.
51. Tavernier, H. L.; Fayer, M. D., Distance Dependence of Electron Transfer in DNA: The Role of the Reorganization Energy and Free Energy. *J. Phys. Chem. B* **2000**, *104*, 11541-11550.
52. Adams, D. M.; Brus, L.; Chidsey, C. E. D.; Creager, S.; Creutz, C.; Kagan, C. R.; Kamat, P. V.; Lieberman, M.; Lindsay, S.; Marcus, R. A.; Metzger, R. M.; Michel-Beyerle, M. E.; Miller, J. R.; Newton, M. D.; Rolison, D. R.; Sankey, O.; Schanze, K. S.; Yardley, J.; Zhu, X. Y., Charge transfer on the nanoscale: Current status. *J. Phys. Chem. B* **2003**, *107*, 6668-6697.

53. ElAyaan, U.; Herlinger, E.; Jameson, R. F.; Linert, W., Anaerobic oxidation of dopamine by iron(III). *J. Chem. Soc. Dalton* **1997**, , 2813-2818.
54. LaVoie, M. J.; Ostaszewski, B. L.; Weihofen, A.; Schlossmacher, M. G.; Selkoe, D. J., Dopamine covalently modifies and functionally inactivates parkin. *Nat. Med.* **2005**, *11*, 1214-1221.
55. Qu, K. G.; Wang, J. S.; Ren, J. S.; Qu, X. G., Carbon Dots Prepared by Hydrothermal Treatment of Dopamine as an Effective Fluorescent Sensing Platform for the Label-Free Detection of Iron(III) Ions and Dopamine. *Chem-Eur J* **2013**, *19*, 7243-7249.

## FIGURES

a)



b)

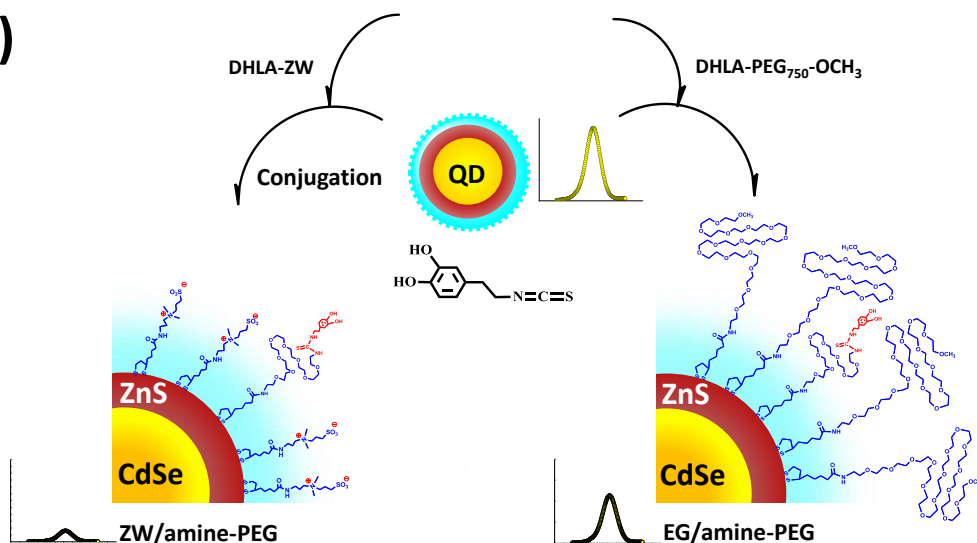


**Figure 1.** (a) Stacked  $^1\text{H}$  NMR spectra collected from LA-PEG- $\text{NH}_2$  ligands with variable PEG size. A pronounced peak at  $\sim 3.5$  ppm was attributed to the protons in the PEG chain. The spectra were collected from ligands dissolved in DMSO. The sharp peak at  $\sim 2.5$ , denoted by \*, is due DMSO in the medium. The plots show that the intensity of the proton peak from PEG moiety increases with the average number of repeat PEG units per ligand. (b) Schematic representation of QD-dopamine conjugate assembly prepared using 5% DHLA-PEG $_{400}$ - $\text{NH}_2$  mixed with either 95% DHLA-ZW, or DHLA-PEG $_{750}$ -methoxy. The insets represent changes in the PL emission.

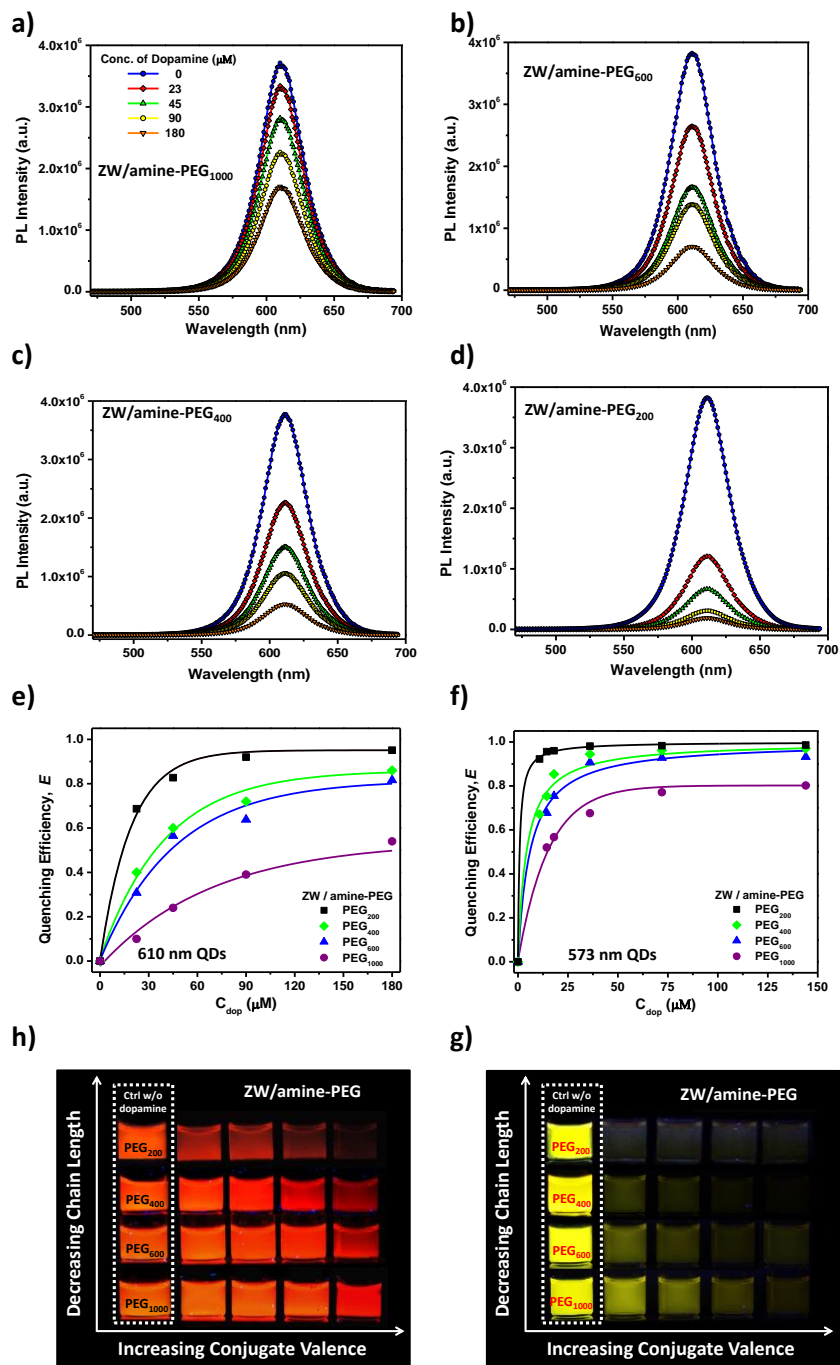


**Figure 2.** (a-d) PL spectra collected from ZW/amine-PEG-QD-dopamine conjugates dispersed in DI water (at pH  $\sim 6.5$ ) for increasing molar concentrations of dopamine-ITC and varying bridge size: (a) PEG<sub>1000</sub>, (b) PEG<sub>600</sub>, (c) PEG<sub>400</sub> and (d) PEG<sub>200</sub>; red-emitting QDs were used. (e) Cumulative plots of the quenching efficiency,  $E$ , versus  $C_{\text{dop}}$  for the above four sets of red-emitting ZW/amine-PEG-QDs. (f) Cumulative plots for  $E$  versus  $C_{\text{dop}}$  for conjugates prepared with the yellow-emitting ZW/amine-PEG-QDs. (g-h) Fluorescence images of selected dispersions of red- and yellow-emitting QD-dopamine conjugates under UV illumination.

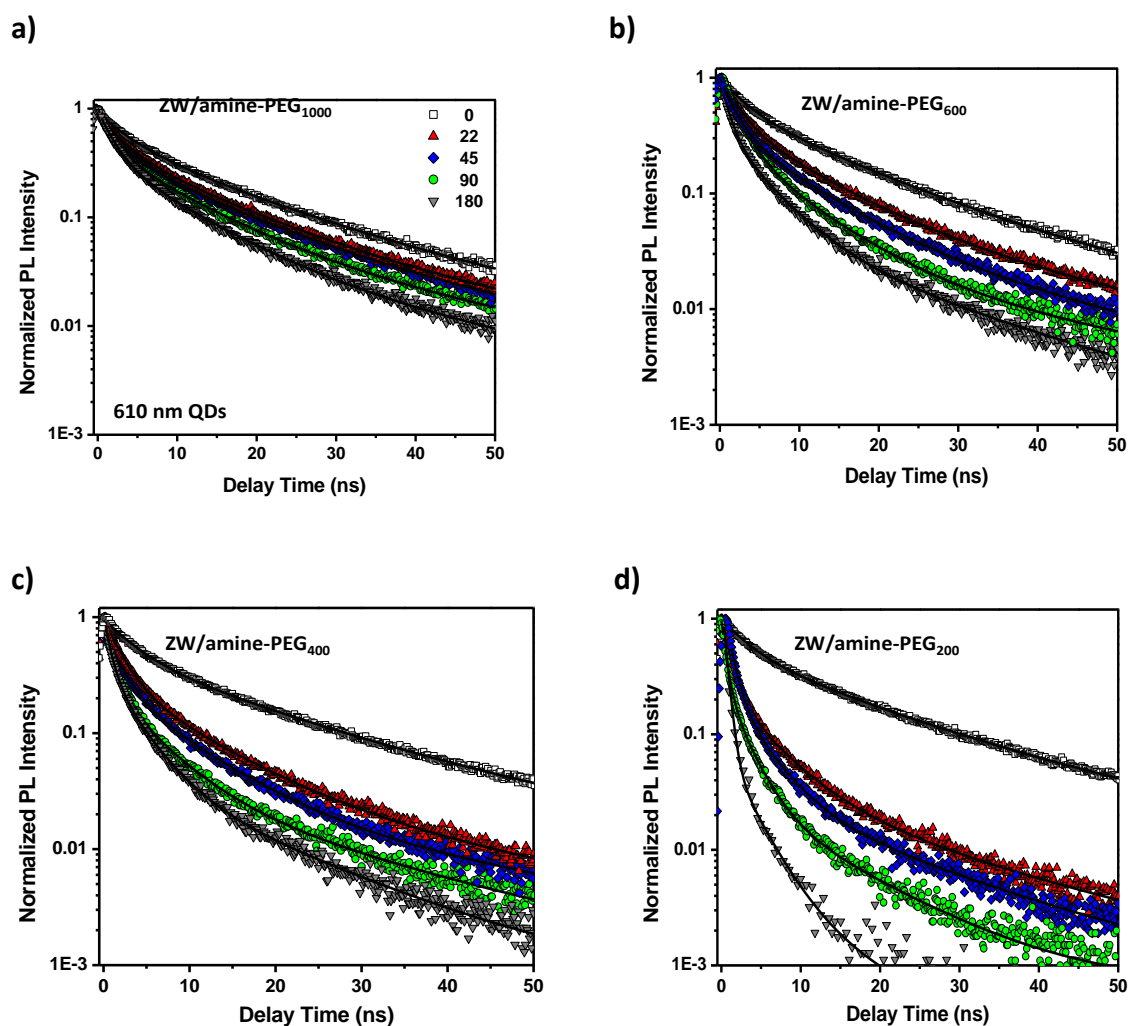


**Figure 3.** Normalized time-resolved PL decay profiles for the conjugates prepared using red-emitting ZW/amine-PEG-QDs with increasing concentration of dopamine-ITC (top to bottom: 0, 22, 45, 90, 180  $\mu\text{M}$ ) for (a) PEG<sub>1000</sub>, (b) PEG<sub>600</sub>, (c) PEG<sub>400</sub> and (d) PEG<sub>200</sub>.

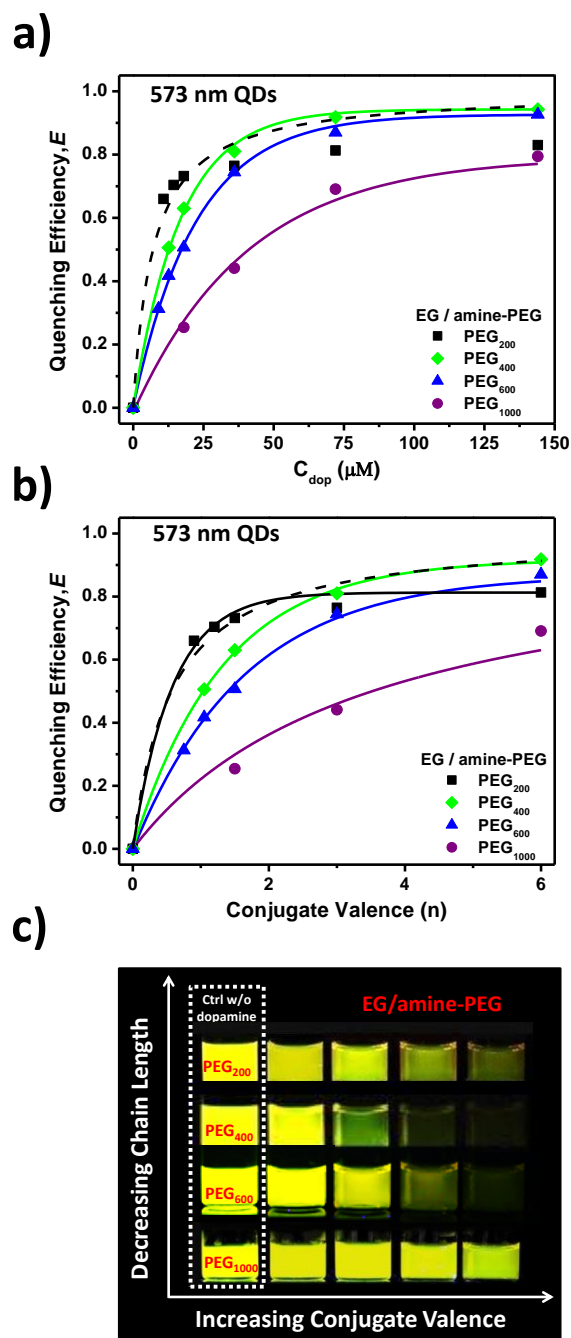


**Figure 4.** (a) Plots of the quenching efficiencies ( $E$  vs  $C_{\text{dop}}$ ) for the various PEG bridges collected from QD-dopamine conjugates prepared using yellow-emitting EG/amine-PEG-QDs along with fits using equation 1 but without accounting for the conjugate heterogeneity. (b) Plots of  $E$  vs valence  $n$  together with fits using eq 2, for PEG<sub>400/600/1000</sub> and fit to eq 3 (accounting for the Poisson correction, dashed line) for PEG<sub>200</sub>. (c) Images of selected dispersions of yellow-emitting QD-dopamine conjugates prepared using EG/amine-PEG-QDs under UV illumination.

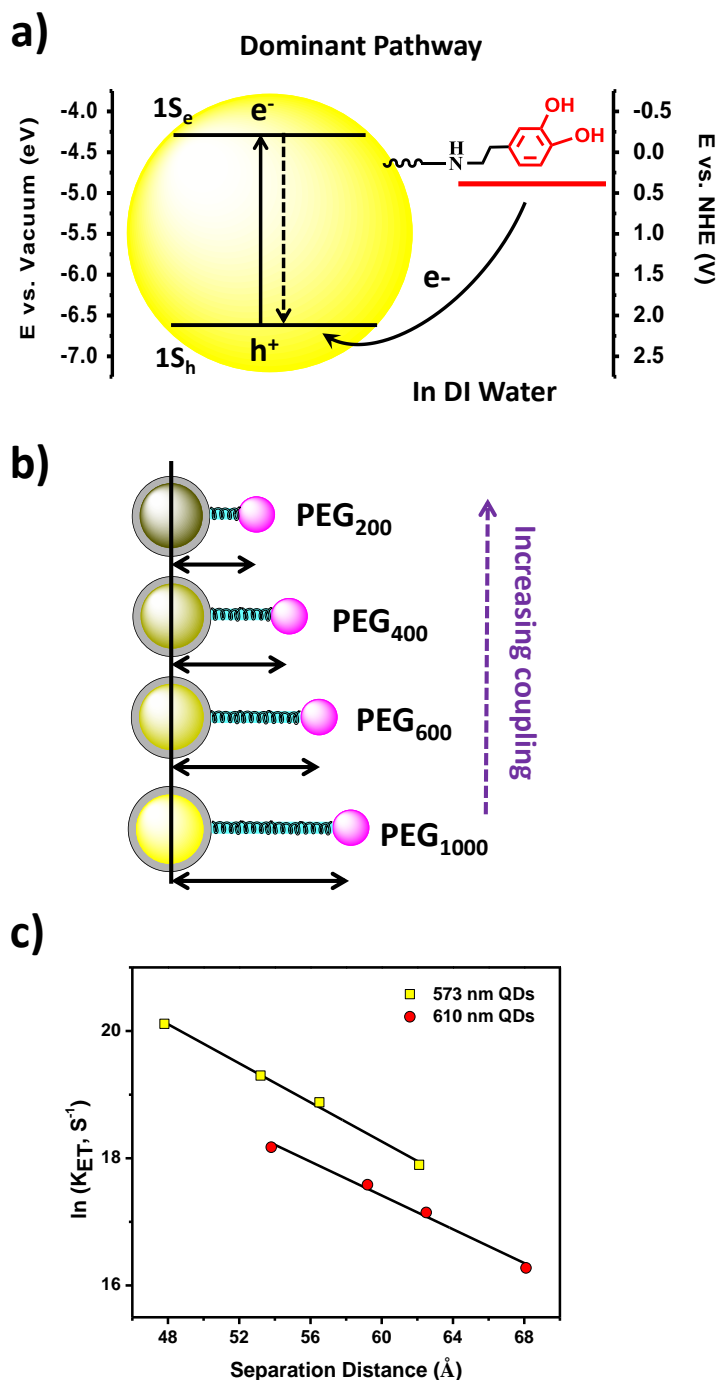


**Figure 5.** (A) Schematic representation of dominant charge transfer interaction pathway between QDs and proximal dopamine in DI water. The redox levels of dopamine at pH 6.5 were extracted from cyclic voltammograms (reported in reference 33) for dispersions of dopamine-PEG-methoxy in buffer media. (B) Schematic representation of the anticipated changes in the separation distance and the corresponding electronic coupling strength ( $H$ ) on the charge transfer interactions. (C) The dependence of electron transfer rate constant versus center-to-center separation distance for yellow- and red-emitting QD-dopamine conjugates prepared using ZW/amine-PEG-QDs. Lines are fit to the data using equation 8.

TOC

